HHS Public Access

Author manuscript

Epilepsy Res. Author manuscript; available in PMC 2017 May 01.

Published in final edited form as:

Epilepsy Res. 2016 May ; 122: 66–72. doi:10.1016/j.eplepsyres.2016.02.010.

Imaging increased glutamate in children with Sturge-Weber syndrome: Association with epilepsy severity

Csaba Juhász[a,b,c], **Jiani Hu**[d], **Yang Xuan**[d], and **Harry T. Chugani**[a,b,c]

[a]Department of Pediatrics, Wayne State University, 3901 Beaubien St., Detroit, Michigan, 48201, USA

[b]Department of Neurology, Wayne State University, 3990 John R. St, Detroit, MI, 48201, USA

[c]PET Center and Translational Imaging Laboratory, Children's Hospital of Michigan, 3901 Beaubien St., Detroit, MI, 48201, USA

[d]Department of Radiology, Harper University Hospital, 3990 John R. St, Detroit, MI, 48201, USA

Abstract

Background—Sturge-Weber syndrome (SWS) is strongly associated with epilepsy. Brain tissue studies have suggested that epileptic activity in SWS is driven by glutamatergic synaptic activity. Here, we used proton magnetic resonance spectroscopic imaging (MRSI) to test if glutamate (GLU) concentrations are increased in the affected hemisphere and if such increases are associated with severity of epilepsy in children with SWS. We also studied the metabolic correlates of MRSI abnormalities, using glucose positron emission tomography (PET) imaging.

Methods—3T MRI and glucose PET were performed in 10 children (age: 7–78 months) with unilateral SWS and a history of epilepsy. MRSI data were acquired from the affected (ipsilateral) and non-affected (contralateral) hemispheres. GLU, N-acetyl-aspartate (NAA) and creatine (Cr) were quantified in multiple voxels; GLU/Cr and NAA/Cr ratios were calculated and compared to seizure frequency as well as glucose PET findings.

Results—The highest GLU/Cr ratios were found in the affected hemisphere in all children except one with severe atrophy. The maximum ipsilateral/contralateral GLU/Cr ratios ranged between 1.0–2.5 (mean: 1.6). Mean ipsilateral/contralateral GLU/Cr ratios were highest in the youngest children and showed a strong positive correlation with clinical seizure frequency scores assessed at the time of the scan (r=0.88, p=0.001) and also at follow-up (up to 1 year, r=0.80, p=0.009). GLU increases in the affected hemisphere coincided with areas showing current or previous increases of glucose metabolism on PET in 5 children. NAA/Cr ratios showed no association with clinical seizure frequency.

Corresponding author: Csaba Juhász, MD, PhD, Professor of Pediatrics and Neurology, Wayne State University School of Medicine, PET Center and Translational Imaging Laboratory, Children's Hospital of Michigan, Wayne State University, 3901 Beaubien St., Detroit, MI, 48201, Phone: (313) 966-5136, juhasz@pet.wayne.edu.

Conflicts of interest: none

Conclusions—Increased glutamate concentrations in the affected hemisphere, measured by MRSI, are common in young children with unilateral SWS and are associated with frequent seizures. The findings lend support to the role of excess glutamate in SWS-associated epilepsy.

Keywords

Sturge-Weber syndrome; epilepsy; MRI; magnetic resonance spectroscopy; glutamate; positron emission tomography

1. INTRODUCTION

Sturge-Weber syndrome (SWS) is a neurocutaneous disorder characterized by a facial capillary malformation (“port wine stain”), leptomeningeal vascular malformation and, in about half of the cases, glaucoma (Bodensteiner, 2010). Intracranial involvement is unilateral in about 85% of SWS cases. A somatic mutation in the G-α q gene, identified both in the port wine stain and affected brain, may be the underlying cause of the SWS vascular abnormalities (Nakashima et al., 2014; Shirley et al., 2013). Neurologic complications, most commonly seizures, motor impairment, and peripheral visual field deficit develop due to the lack of proper cortical venous drainage, leading to venous stasis, hypoxia and tissue damage in affected brain regions.

SWS is strongly associated with epilepsy: up to 80% of SWS patients develop seizures, which most commonly start during the first 1–2 years of life (Comi, 2010; Lo et al., 2012; Sujansky and Conradi, 1995). Early seizure onset and medically refractory epilepsy are associated with poor cognitive outcome (Jagtap et al., 2013; Pascual-Castroviejo et al., 2008). In such patients, surgical resection (hemispherectomy or focal resection) can be highly effective in controlling the seizures and, possibly, prevent or reverse cognitive decline (Bourgeois et al., 2007; Kossoff et al., 2002). However, seizure outcome and associated neuro-cognitive decline cannot be predicted based on clinical or conventional imaging criteria at the early disease stages.

SWS intracranial involvement is most commonly evaluated by contrast-enhanced MRI, which can detect the leptomeningeal venous malformation, deep venous abnormalities, atrophy, calcification and other associated brain abnormalities (Juhasz, 2010; Lo et al., 2012). Functional imaging studies, such as glucose positron emission tomography (PET), can be useful clinically in selected SWS patients as part of the evaluation for epilepsy surgery. Decreased glucose metabolism detected in the affected hemisphere(s) can extend beyond structural brain abnormalities depicted by CT and MRI (Alkonyi et al., 2012; Chugani et al., 1989). However, a subset of young children with SWS show paradoxically increased glucose metabolism in the affected hemisphere on interictal PET both before and after the onset of the first clinical seizure(s) (Chugani et al., 1989; Alkonyi et al., 2011). Such hypermetabolic cortical regions were most commonly observed shortly (within months) before and/or after the onset of the first clinical seizure(s) (Alkonyi et al., 2011), i.e., during the presumed period of epileptogenesis (Dudek and Staley, 2011).

The pathophysiology of SWS-associated epilepsy and the role of these transient metabolic changes in SWS epileptogenesis remain poorly understood. One plausible mechanism

involves the role of excess glutamate (GLU) released due to chronic hypoxia; indeed, excessive stimulation of glutamate receptors in the affected brain could facilitate seizures and also lead to excitotoxic brain injury (Johnston, 2005; Kostandy, 2012). Tissue studies have shown that epileptiform activity in affected SWS cortex is driven by glutamatergic synapses (Tyzio et al., 2009).

Advances in ^{1}H-magnetic resonance spectroscopic imaging (^{1}H-MRSI) allow non-invasive measurement of cerebral GLU concentrations in multiple voxels simultaneously (Hu et al., 2007; Yang et al., 2008). In a recent study using GLU chemical exchange saturation transfer imaging in patients with temporal lobe epilepsy, increased glutamate was invariably found in the epileptic temporal lobe (Davis et al., 2015). In the present study, we utilized GLU ^{1}H-MRSI to test if children with unilateral SWS show increased GLU levels in the affected (epileptic) hemisphere as compared to the unaffected side. We also evaluated if GLU abnormalities, measured by ^{1}H-MRSI, are related to severity of clinical epilepsy. Finally, we evaluated glucose metabolic correlates of ^{1}H-MRSI GLU asymmetries using PET imaging.

2. MATERIAL AND METHODS

Ten children with SWS (8 girls, 2 boys, age: 7–78 months; mean: 35 months) were prospectively enrolled in a clinical neuroimaging research study (Table 1). All 10 children had a history of seizures and unilateral SWS brain involvement in the form of a leptomeningeal venous malformation detected by contrast-enhanced MRI. All 10 children underwent a 3T MRI with MRSI and 2-deoxy-2[^{18}F]fluoro-D-glucose (FDG)-PET performed with scalp EEG monitoring during the uptake period; typically, MRI and PET studies were performed on consecutive days. All children were on at least one antiepileptic medication (Table 1). Clinical seizure frequency was evaluated by parent interviews and medical charts, and a seizure frequency score was assigned to each patient based on clinical seizures occurring during the one year period prior to the imaging study (or since seizure onset, if seizures started less than one year before the study). The scoring system was slightly modified from a previous study on children with SWS (Behen et al., 2011), and the scores were determined as follows: 0=no seizure in the last 1 year; 1: 1–11 seizures per year; 2: 1–4 seizures per month; 3: >4 seizures per month. Similar scores were also determined at follow-up, i.e., 1 year after baseline or at the time of epilepsy surgery, if surgery was done within one year after the baseline studies (Table 1). Epilepsy surgery was performed in two children (#2 and #5, 6 and 3 months after the imaging studies, respectively). The study was approved by the Human Investigation Committee at Wayne State University, and written informed consent of the parent or legal guardian was obtained.

2.1. MRI studies

All MRI studies have been performed on a Siemens MAGNETOM Verio 3T scanner (Siemens Medical Solutions, Erlangen) located at the Harper University Hospital, Detroit Medical Center. The MRI protocol included an axial T1 3D Magnetization Prepared Rapid Gradient Echo (MPRAGE) with 1mm slice thickness, axial T2 turbo spin-echo, axial T2/fluid-attenuated inversion recovery (FLAIR), susceptibility weighted imaging (SWI) and diffusion tensor imaging. During bolus-injection of Gadolinium-diethylene triamine

pentaacetic acid (DTPA; dose: 0.1 mmol/kg of body weight), dynamic contrast enhanced MR perfusion-weighted imaging was acquired, followed by a post-contrast axial 3D MPRAGE image.

2.2. ^{1}H-MR Spectroscopic Imaging

In addition to the above MRI sequences, all children underwent MR spectroscopic imaging using a chemical shift imaging (CSI) Stimulated Echo Acquisition Sequence (STEAM) to acquire 2D spectroscopic data (TR=1500 ms, TE=40 ms, TM=8 ms, voxel size=15mm×15mm×15mm, NA=16). The 15 mm thick slabs were placed on the axial T1 image, in most cases covering portions of the frontal and parietal lobes above the level of the lateral ventricles, including brain regions with apparent SWS brain involvement (Figure 1). In two children, the level of the slab was lowered in order to cover temporal and occipital lobes, because of the location of the main SWS brain abnormalities. Each slab included voxels covering some cortex and subcortical white matter. ^{1}H MRS spectra were post-processed using the MRS analysis software package LCModel (V6.0, S. Provencher; Ontario, Canada) implemented on a PC with a Linux operating system, which allows quantification of the metabolites (Provencher, 1993). GLU concentrations were calculated for each voxel after quality control (Hu et al., 2007; Yang et al., 2008); voxels with poor spectral quality were excluded. Figure 1B shows a typical spectrum with glutamate (GLU) and glutamine (GLN) peaks indicated, along with NAA, choline and creatine (Cr) peaks. GLU/Cr ratios were then calculated for each voxel both ipsi- and contralateral to the SWS brain involvement (Figure 1C). An average of 27 voxels were evaluated per patient (range: 14–36 voxels).

2.3. FDG-PET

The details of FDG-PET acquisition and data analysis have been described previously (Alkonyi et al., 2011). In brief, all PET scans were acquired using an EXACT/HR PET scanner (CTI/Siemens, Hoffman Estates, IL, U.S.A.), which provides simultaneous acquisition of 47 contiguous transaxial images with a slice thickness of 3.125 mm. The reconstructed image resolution was 5.5 ± 0.35 mm at full width at half-maximum (FWHM) in-plane and 6.0 ± 0.49 mm at FWHM in the axial direction. Scalp EEG was monitored in all children during the tracer uptake period. 0.143 mCi/kg of FDG was injected intravenously as a slow bolus followed by a 30-min uptake period. Forty minutes after injection, a static 20-min emission scan was acquired. Calculated attenuation correction was applied to the images using automated threshold fits to the sinogram data. Based on the EEG data and clinical observation, all PET scans were acquired in the interictal state.

2.4. Sedation during imaging studies

Sedation was applied in all children during the MRI studies and during the scanning (but not uptake) phase of the PET studies; thus, sedation had no effect on the glucose uptake pattern. Children were sedated with pentobarbital (1.5–3 mcg/kg) and midazolam (0.1–0.2 mcg/kg); or by midazolam (0.1–0.2 mcg/kg) followed by dexmedetomidine (1–2 mcg/kg), titrated slowly to achieve mild to moderate sedation. In some cases, fentanyl (1 mcg/kg) was used as necessary in conjunction with either pentobarbital or midazolam. All sedated children were continuously monitored by a physician and a pediatric nurse, and physiologic parameters

(heart rate, pulse oximetry, respiration) were measured during the entire length of the imaging studies.

2.5. Statistical analysis

Mean GLU/Cr and NAA/Cr ratios were calculated in each (ipsilateral [affected] and contralateral) hemisphere by averaging these ratios across all voxels in the hemispheres. Spearman's rank correlation and multivariate regression analysis were used to assess the correlations between age, seizure frequency scores, NAA/Cr and GLU/Cr ratios and their ipsilateral/contralateral ratios. $P<0.05$ was considered to be significant.

3. RESULTS

3.1. GLU/Cr and NAA/Cr ratios

In 9 out of the 10 patients, the voxel with the highest GLU/Cr ratio was found in the affected hemisphere. The only exception was patient #9 (Table 1), a 5-year 5-month old girl with extensive right hemispheric atrophy, who had been seizure-free for more than a year. For the 10 patients, Ipsilateral/contralateral ratios in the voxels with the highest GLU/Cr ranged between 1.0 and 2.5 (mean: 1.63; Table 2). The voxel locations of the highest GLU/Cr ratios in the affected hemisphere varied across patients and occurred in the frontal (n=5), parietal (n=3) and temporal lobe (n=2) (Table 2).

Mean GLU/Cr ratios were higher in the affected hemisphere (as compared to the contralateral side) in 7 of the 8 youngest children, who all had seizures in the previous one year; while the two oldest children (patients #9 and 10) with no seizures in the previous one year had lower mean GLU/Cr ratios in the affected hemisphere as compared to the contralateral side (Table 2). In contrast, mean NAA/Cr ratios in the affected hemisphere were lower in five, slightly higher in three patients, while they were symmetric (ipsilateral/ contralateral ratios 1.0) in two (Table 2).

3.2. Correlations between MRSI variables and clinical epilepsy variables

High mean ipsilateral/ contralateral ratios of GLU/Cr (but not NAA/Cr) were strongly associated with high seizure frequency scores assessed both at baseline (r-0.88, p=0.001) and at follow-up (r=0.80, p=0.009) (Table 3; Figure 2). Younger age at baseline was also associated with higher mean GLU/Cr ipsilateral/contralateral ratios (p=0.048, Table 3). In a multivariate regression analysis, however, only seizure frequency, but not age, was associated with GLU/Cr ratios (partial correlations: seizure frequency: r=0.82, p=0.007; age: r=−0.26, p=0.50).

3.3. GLU/Cr and glucose metabolic abnormalities

The area showing the highest GLU/Cr value in the affected hemisphere showed increased glucose metabolism on PET in the 3 youngest children (see example on Figure 1) and decreased metabolism in the other 7; however, two of these 7 patients (#6 and #8) had a previous FDG PET one year earlier, which showed a (transient) increased glucose metabolism involving the area with the highest GLU/Cr values.

4. DISCUSSION

This study has three main findings: First, we have shown consistently higher GLU/Cr ratios in the affected hemisphere in children with unilateral SWS; no similar increases were found in NAA/Cr ratios measured in the same brain regions, indicating that the observed increases were GLU-specific. Second, high mean GLU/Cr asymmetries were associated with frequent seizures both at the time of imaging and at follow-up, suggesting that increased GLU concentrations in the affected hemisphere is related to epilepsy severity. Finally, brain regions with increased GLU/Cr showed either increased (present in younger SWS children) or decreased interictal glucose metabolism on PET. Altogether, these findings support a role of abnormal glutamatergic activity in SWS-associated clinical epilepsy.

4.1. Higher glutamate in the epileptic hemisphere

Our results provide compelling imaging data for increased GLU concentrations in the affected hemisphere of children with SWS, as compared to the unaffected side. The most plausible explanation for these higher GLU levels in affected brain regions is the excess release and accumulation of extracellular GLU as a result of chronic hypoxia due to insufficient venous drainage. Previous studies have indeed shown that perinatal hypoxia can lead to excessive stimulation of glutamate receptors along with the down-regulation of glutamate decarboxylase genes, thus leading to increased GLU levels and contributing to cell injury and high susceptibility to seizures (Johnston, 2005). In newborn rats exposed to hypoxia, decreased GLU uptake by astroglial cells has led to increased levels of extracellular GLU, thus contributing to hypoxia-induced oligodendroglia death and white matter injury (Murugan et al., 2013). This mechanism may play a role in the previously reported white matter damage and atrophy in the affected hemisphere of children with SWS (Juhasz et al., 2007). Increased GLU concentrations, measured by MRS, have also been reported in epileptogenic cortical developmental malformations (Simister et al., 2007); recent histopathology studies demonstrated that such malformations (particularly focal cortical dysplasia and polymicrogyria) are frequently associated with SWS, although they may not be readily identified on MRI (Pinto et al., 2015; Wang et al., 2015). Thus, such malformations may also be a potential source of elevated GLU in SWS.

Since a significant proportion of energy metabolism of the brain is utilized for glutamatergic synaptic activity and GLU recycling (Pellerin and Magistretti, 1994; Schousboe et al., 2007; Shulman et al., 2004; Sibson et al., 1998), increased GLU may also induce increased glucose metabolism, which can be measured by FDG-PET. Indeed, in our study increased FDG uptake on PET was observed in 5 of the 9 patients showing higher GLU/Cr values in the affected hemisphere, involving the same lobar regions. Interestingly, in two of these cases, hypermetabolism was seen on a previous PET scan and switched to decreased metabolism by the time of the MRSI study. GLU/Cr ratios were the highest in young SWS children, similar to the age distribution of increased glucose metabolism, which had been observed most commonly in young SWS children with a mean age of 1.9 years (as opposed to 4.5 years showing decreased metabolism on PET) (Alkonyi et al., 2011).

Altogether, despite the cross-sectional design, our results suggest that GLU increases may peak early during the SWS disease course but can persist even after the affected region

becomes hypometabolic, which almost invariably occurred in previous, longitudinal PET studies (Alkonyi et al., 2011; Chugani et al., 1989). Coincidence of increased GLU and interictal hypermetabolism in the young SWS brain suggests a causal link between these two during a critical developmental period. This mechanism is likely operational not only in SWS but also in infants following perinatal hypoxia where, similar to SWS, both high GLU concentrations and transient glucose hypermetabolism were observed in the basal ganglia (Batista et al., 2007; Pu et al., 2000). Taken together, these data support a link between hypoxia-induced GLU release, increased metabolism and excitotoxicity leading to subsequent neuronal damage and eventual hypometabolism associated with brain atrophy, thus providing a plausible pathomechanism of progressive brain damage in SWS.

4.2. Potential clinical implications

Our findings suggest that GLU MRS imaging may be useful in the clinical setting to evaluate risk for severe epilepsy in children with SWS. While PET is not feasible for most SWS patients with recent-onset seizures, GLU MRSI can be incorporated in clinical MRI protocols. High GLU/Cr ratios in the affected hemisphere may indicate a high risk for intractable seizures, thus prompting tight follow-up or adjustment of anti-epileptic treatment, and possibly early surgery. Our data also suggest that drugs acting upon the glutamatergic system may be effective not only to prevent seizures but perhaps to halt GLU-induced excitotoxic brain damage in SWS. Although most currently used drugs do not directly affect the GLU receptors, new-generation AMPA (α-amino-3-hydroxy-5-methyl-4-isoxazolepropionic acid) receptor antagonists, such as perampanel, can inhibit GLU-mediated excitation, and may be considered for SWS epilepsy treatment in the future as clinical experience with such drugs becomes available in pediatric populations (Biro et al., 2015; Rosenfeld et al., 2015). Another therapeutic option would involve inhibition of mammalian target of rapamycin (mTOR) complex 1 signaling that may not only reverse increases of glutamatergic neurotransmission (Talos et al., 2012) but could also be beneficial to treat the vascular malformation (Marques et al., 2015; Shirazi et al., 2007).

4.3. Methodological considerations and limitations

Our study has methodological novelties but also limitations. The main novelty is the use of a multivoxel CSI approach that can separate GLU from the GLN peak reliably, as validated in previous studies (Hu et al., 2007; Yang et al., 2008). Previous multivoxel MRS studies in human epilepsy mostly relied on the assessment of Glx, which incorporates both GLU and GLN peaks, but cannot measure GLU separately (Simister et al., 2002; Woermann et al., 2001). However, microdialysis studies showed the selective increase of GLU (but not GLN) in the epileptogenic hippocampus and cortex (Cavus et al., 2005; Pan et al., 2008); therefore, selective GLU measurement *in vivo* provides more specific information regarding epileptogenicity.

Limitations of MRSI include the limited brain sampling, which makes it impossible to explore the entire supratentorial brain. We sampled the hemispheres above the level of the lateral ventricles in most cases, thus including voxels mostly from the frontal and parietal lobes, except in cases where the leptomeningeal malformation was predominantly temporo-occipital, where the MRSI slab was lower.

A further limitation of this technique is the difficulty of including pure cortical regions due to the relatively large voxel sizes, and because cortex in the vicinity of the skull is prone to artifacts; therefore, most voxels contained both cortex and subcortical white matter. Still, the use of mean values across multiple voxels in each hemisphere provided a relatively robust measure of the GLU peaks. Importantly, we relied on asymmetries (ipsilateral/contralateral ratios), which is a common methodological approach in pediatric imaging studies, where age-matched healthy control values are difficult to obtain, and non-linear developmental variations of imaging parameters are common. This approach is useful in unilateral lesions (i.e., the majority of SWS cases), where the use of the normal (unaffected) hemisphere as an internal control is valid. Although the physiologic asymmetries of GLU concentrations have not been established in children, the observed asymmetries in unilateral SWS are unlikely due to physiologic asymmetries, considering the consistent occurrence of the highest values in the affected hemisphere and the robust correlation of asymmetries of asymmetries with clinical seizure frequency.

Finally, the study population was small, which is a common problem in single-center studies of rare disorders. Nevertheless, this study provides proof-of-principle data for the feasibility of detecting increased GLU concentrations in the affected hemisphere in SWS. Further validation of this imaging marker in SWS-associated epileptogenesis, or epilepsies of other etiologies, will likely require multi-center studies using a standardized MRI/MRS protocol.

4.4. Conclusions

These data demonstrate that increased GLU is common in the affected hemisphere of children with unilateral SWS and epilepsy. High asymmetries of mean GLU/Cr ratios are associated with frequent seizures. Areas with high GLU can show increased (but also decreased) interictal glucose metabolism on PET. Altogether, the findings lend support to the role of excess GLU in SWS-associated epileptogenesis and suggest that anti-glutamatergic treatment may be useful to alleviate seizures in this group of patients.

Acknowledgments

We thank Cathie Germain, MA, and Cynthia Burnett, BA, for assisting patient recruitment and scheduling; Jane Cornett, RN and Anne Deboard, RN, for performing sedation for imaging. We are also grateful to the Sturge-Weber Foundation and the families who participated in these studies. This study was partially funded by a grant from the National Institutes of Health (R01 NS041922 to C.J.).

REFERENCES

Alkonyi B, Chugani HT, Juhasz C. Transient focal cortical increase of interictal glucose metabolism in Sturge-Weber syndrome: implications for epileptogenesis. Epilepsia. 2011; 52:1265–1272. [PubMed: 21480889]

Alkonyi B, Miao Y, Wu J, Cai Z, Hu J, Chugani HT, Juhasz C. A perfusion-metabolic mismatch in Sturge-Weber syndrome: a multimodality imaging study. Brain & Development. 2012; 34:553–562. [PubMed: 22075184]

Batista CE, Chugani HT, Juhasz C, Behen ME, Shankaran S. Transient hypermetabolism of the basal ganglia following perinatal hypoxia. Pediatric Neurology. 2007; 36:330–333. [PubMed: 17509466]

Behen ME, Juhasz C, Wolfe-Christensen C, Guy W, Halverson S, Rothermel R, Janisse J, Chugani HT. Brain damage and IQ in unilateral Sturge-Weber syndrome: support for a "fresh start" hypothesis. Epilepsy & Behavior : E&B. 2011; 22:352–357.

Biro A, Stephani U, Tarallo T, Bast T, Schlachter K, Fleger M, Kurlemann G, Fiedler B, Leiz S, Nikanorova M, Wolff M, Muller A, Selch C, Staudt M, Kluger G. Effectiveness and tolerability of perampanel in children and adolescents with refractory epilepsies: first experiences. Neuropediatrics. 2015; 46:110–116. [PubMed: 25730374]

Bodensteiner, J.; Roach, ES. Overview of Sturge-Weber syndrome. In: Bodensteiner, JB.; Roach, ES., editors. Sturge-Weber syndrome. 2nd. Mt. Freedom, NJ: The Sturge-Weber Foundation; 2010. p. 19-32.

Bourgeois M, Crimmins DW, de Oliveira RS, Arzimanoglou A, Garnett M, Roujeau T, Di Rocco F, Sainte-Rose C. Surgical treatment of epilepsy in Sturge-Weber syndrome in children. Journal of Neurosurgery. 2007; 106:20–28. [PubMed: 17233308]

Cavus I, Kasoff WS, Cassaday MP, Jacob R, Gueorguieva R, Sherwin RS, Krystal JH, Spencer DD, Abi-Saab WM. Extracellular metabolites in the cortex and hippocampus of epileptic patients. Annals of Neurology. 2005; 57:226–235. [PubMed: 15668975]

Chugani HT, Mazziotta JC, Phelps ME. Sturge-Weber syndrome: a study of cerebral glucose utilization with positron emission tomography. The Journal of Pediatrics. 1989; 114:244–253. [PubMed: 2783735]

Comi, A. Neurological manifestations of Sturge-Weber syndrome. In: Bodensteiner, J.; Roach, ES., editors. Sturge-Weber syndrome. 2nd. Mt. Freedom, NJ: The Sturge-Weber Foundation; 2010. p. 69-93.

Davis KA, Nanga RP, Das S, Chen SH, Hadar PN, Pollard JR, Lucas TH, Shinohara RT, Litt B, Hariharan H, Elliott MA, Detre JA, Reddy R. Glutamate imaging (GluCEST) lateralizes epileptic foci in nonlesional temporal lobe epilepsy. Science Translational Medicine. 2015; 7:309ra161.

Dudek FE, Staley KJ. The time course of acquired epilepsy: implications for therapeutic intervention to suppress epileptogenesis. Neuroscience letters. 2011; 497:240–246. [PubMed: 21458536]

Hu J, Yang S, Xuan Y, Jiang Q, Yang Y, Haacke EM. Simultaneous detection of resolved glutamate, glutamine, and gamma-aminobutyric acid at 4T. Journal of Magnetic Resonance. 2007; 185:204–213. [PubMed: 17223596]

Jagtap S, Srinivas G, Harsha KJ, Radhakrishnan N, Radhakrishnan A. Sturge-Weber syndrome: clinical spectrum, disease course, and outcome of 30 patients. Journal of Child Neurology. 2013; 28:725–731. [PubMed: 22832777]

Johnston MV. Excitotoxicity in perinatal brain injury. Brain Pathology. 2005; 15:234–240. [PubMed: 16196390]

Juhasz, C. Imaging brain structure and function in Sturge-Weber syndrome. In: Bodensteiner, JB.; Roach, ES., editors. Sturge-Weber syndrome. 2nd. Mt. Freedom, NJ: The Sturge-Weber Foundation; 2010. p. 109-148.

Juhasz C, Lai C, Behen ME, Muzik O, Helder EJ, Chugani DC, Chugani HT. White matter volume as a major predictor of cognitive function in Sturge-Weber syndrome. Archives of Neurology. 2007; 64:1169–1174. [PubMed: 17698708]

Kossoff EH, Buck C, Freeman JM. Outcomes of 32 hemispherectomies for Sturge- Weber syndrome worldwide. Neurology. 2002; 59:1735–1738. [PubMed: 12473761]

Kostandy BB. The role of glutamate in neuronal ischemic injury: the role of spark in fire. Neurological Sciences. 2012; 33:223–237. [PubMed: 22044990]

Lo W, Marchuk DA, Ball KL, Juhasz C, Jordan LC, Ewen JB, Comi A. Brain Vascular Malformation Consortium National Sturge-Weber Syndrome, W. Updates and future horizons on the understanding, diagnosis, and treatment of Sturge-Weber syndrome brain involvement. Developmental Medicine and Child Neurology. 2012; 54:214–223. [PubMed: 22191476]

Marques L, Nunez-Cordoba JM, Aguado L, Pretel M, Boixeda P, Nagore E, Baselga E, Redondo P. Topical rapamycin combined with pulsed dye laser in the treatment of capillary vascular malformations in Sturge-Weber syndrome: phase II, randomized, double-blind, intraindividual placebo-controlled clinical trial. Journal of the American Academy of Dermatology. 2015; 72:151–158. e151. [PubMed: 25455610]

Murugan M, Ling EA, Kaur C. Dysregulated glutamate uptake by astrocytes causes oligodendroglia death in hypoxic perventricular white matter damage. Molecular and Cellular Neurosciences. 2013; 56:342–354. [PubMed: 23859823]

Nakashima M, Miyajima M, Sugano H, Iimura Y, Kato M, Tsurusaki Y, Miyake N, Saitsu H, Arai H, Matsumoto N. The somatic GNAQ mutation c.548G>A (p.R183Q) is consistently found in Sturge-Weber syndrome. Journal of Human Genetics. 2014; 59:691–693. [PubMed: 25374402]

Pan JW, Williamson A, Cavus I, Hetherington HP, Zaveri H, Petroff OA, Spencer DD. Neurometabolism in human epilepsy. Epilepsia. 2008; 49(Suppl 3):31–41. [PubMed: 18304254]

Pascual-Castroviejo I, Pascual-Pascual SI, Velazquez-Fragua R, Viano J. Sturge-Weber syndrome: study of 55 patients. The Canadian Journal of Neurological Sciences. 2008; 35:301–307. [PubMed: 18714797]

Pellerin L, Magistretti PJ. Glutamate uptake into astrocytes stimulates aerobic glycolysis: a mechanism coupling neuronal activity to glucose utilization. Proceedings of the National Academy of Sciences of the United States of America. 1994; 91:10625–10629. [PubMed: 7938003]

Pinto AL, Chen L, Friedman R, Grant PE, Poduri A, Takeoka M, Prabhu SP, Sahin M. Sturge-Weber Syndrome: Brain Magnetic Resonance Imaging and Neuropathology Findings. Pediatric Neurology. 2015 Nov 26. 2015 pii: S0887-8994(15)30029-1.

Provencher SW. Estimation of metabolite concentrations from localized in vivo proton NMR spectra. Magnetic Resonance in Medicine. 1993; 30:672–679. [PubMed: 8139448]

Pu Y, Li QF, Zeng CM, Gao J, Qi J, Luo DX, Mahankali S, Fox PT, Gao JH. Increased detectability of alpha brain glutamate/glutamine in neonatal hypoxic-ischemic encephalopathy. AJNR. American Journal of Neuroradiology. 2000; 21:203–212. [PubMed: 10669252]

Rosenfeld W, Conry J, Lagae L, Rozentals G, Yang H, Fain R, Williams B, Kumar D, Zhu J, Laurenza A. Efficacy and safety of perampanel in adolescent patients with drug-resistant partial seizures in three double-blind, placebo-controlled, phase III randomized clinical studies and a combined extension study. European Journal of Paediatric Neurology. 2015; 19:435–445. [PubMed: 25823975]

Schousboe A, Bak LK, Sickmann HM, Sonnewald U, Waagepetersen HS. Energy substrates to support glutamatergic and GABAergic synaptic function: role of glycogen, glucose and lactate. Neurotoxicity Research. 2007; 12:263–268. [PubMed: 18201953]

Shirazi F, Cohen C, Fried L, Arbiser JL. Mammalian target of rapamycin (mTOR) is activated in cutaneous vascular malformations in vivo. Lymphatic Research and Biology. 2007; 5:233–236. [PubMed: 18370913]

Shirley MD, Tang H, Gallione CJ, Baugher JD, Frelin LP, Cohen B, North PE, Marchuk DA, Comi AM, Pevsner J. Sturge-Weber syndrome and port-wine stains caused by somatic mutation in GNAQ. The New England Journal of Medicine. 2013; 368:1971–1979. [PubMed: 23656586]

Shulman RG, Rothman DL, Behar KL, Hyder F. Energetic basis of brain activity: implications for neuroimaging. Trends in Neurosciences. 2004; 27:489–495. [PubMed: 15271497]

Sibson NR, Dhankhar A, Mason GF, Rothman DL, Behar KL, Shulman RG. Stoichiometric coupling of brain glucose metabolism and glutamatergic neuronal activity. Proceedings of the National Academy of Sciences of the United States of America. 1998; 95:316–321. [PubMed: 9419373]

Simister RJ, McLean MA, Barker GJ, Duncan JS. Proton magnetic resonance spectroscopy of malformations of cortical development causing epilepsy. Epilepsy Research. 2007; 74:107–115. [PubMed: 17379481]

Simister RJ, Woermann FG, McLean MA, Bartlett PA, Barker GJ, Duncan JS. A short-echo-time proton magnetic resonance spectroscopic imaging study of temporal lobe epilepsy. Epilepsia. 2002; 43:1021–1031. [PubMed: 12199727]

Sujansky E, Conradi S. Sturge-Weber syndrome: age of onset of seizures and glaucoma and the prognosis for affected children. Journal of Child Neurology. 1995; 10:49–58. [PubMed: 7769179]

Talos DM, Sun H, Zhou X, Fitzgerald EC, Jackson MC, Klein PM, Lan VJ, Joseph A, Jensen FE. The interaction between early life epilepsy and autistic-like behavioral consequences: a role for the mammalian target of rapamycin (mTOR) pathway. PloS One. 2012; 7:e35885. [PubMed: 22567115]

Tyzio R, Khalilov I, Represa A, Crepel V, Zilberter Y, Rheims S, Aniksztejn L, Cossart R, Nardou R, Mukhtarov M, Minlebaev M, Epsztein J, Milh M, Becq H, Jorquera I, Bulteau C, Fohlen M, Oliver V, Dulac O, Dorfmuller G, Delalande O, Ben-Ari Y, Khazipov R. Inhibitory actions of the gamma-

aminobutyric acid in pediatric Sturge-Weber syndrome. Annals of Neurology. 2009; 66:209–218. [PubMed: 19743469]

Wang DD, Blumcke I, Coras R, Zhou WJ, Lu DH, Gui QP, Hu JX, Zuo HC, Chen SY, Piao YS. Sturge-Weber Syndrome Is Associated with Cortical Dysplasia ILAE Type IIIc and Excessive Hypertrophic Pyramidal Neurons in Brain Resections for Intractable Epilepsy. Brain Pathology. 2015; 25:248–255. [PubMed: 25040707]

Woermann FG, McLean MA, Bartlett PA, Barker GJ, Duncan JS. Quantitative short echo time proton magnetic resonance spectroscopic imaging study of malformations of cortical development causing epilepsy. Brain. 2001; 124:427–436. [PubMed: 11157569]

Yang S, Hu J, Kou Z, Yang Y. Spectral simplification for resolved glutamate and glutamine measurement using a standard STEAM sequence with optimized timing parameters at 3, 4, 4.7, 7, and 9.4T. Magnetic Resonance in Medicine. 2008; 59:236–244. [PubMed: 18228589]

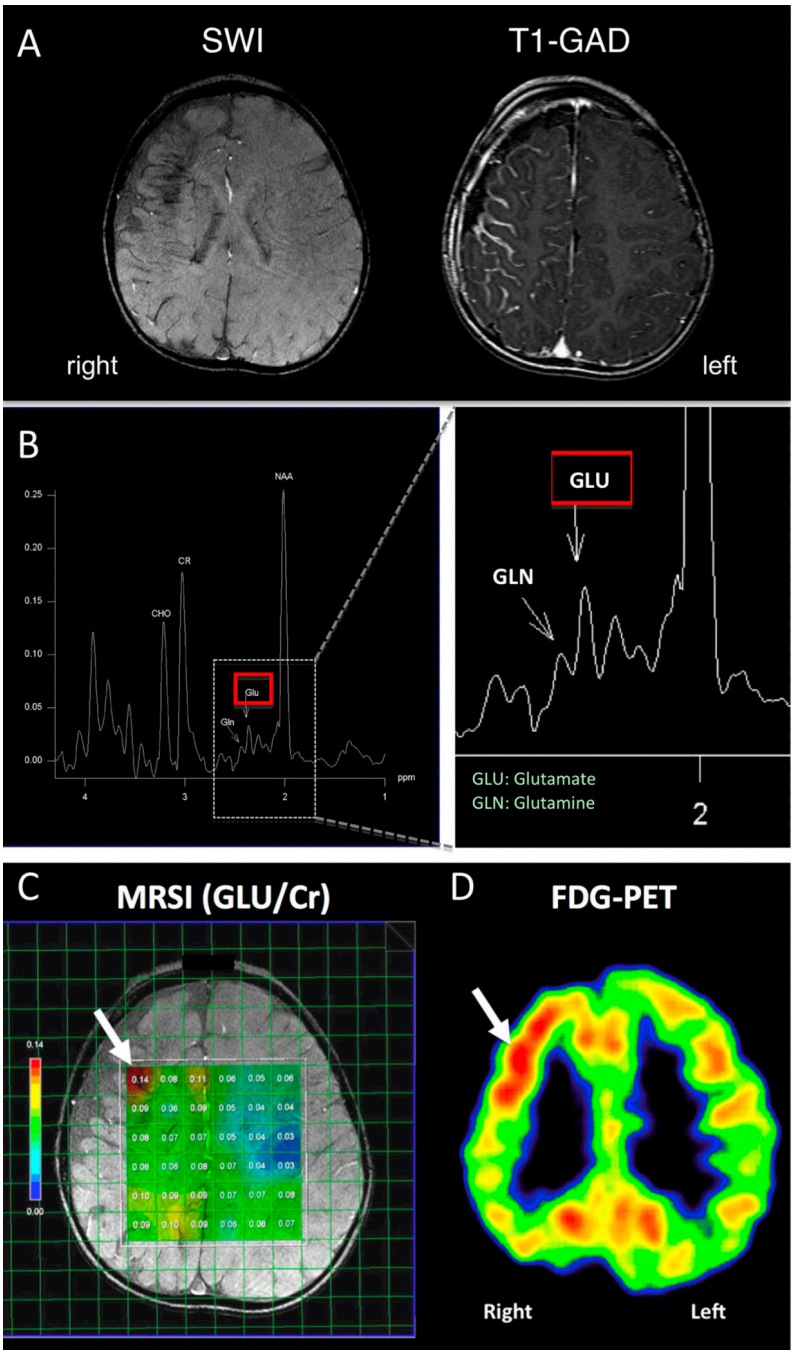

Figure 1.

(A) Susceptibility-weighted imaging (SWI) and post-gadolinium T1-weighted MR image (T1-GAD) of a young child (patient #2) with right hemispheric SWS involvement. SWI showed right frontal lobe atrophy, deep transmedullary veins and signs of calcification in the fronto-parietal region; T1-GAD demonstrated right hemispheric leptomeningeal enhancement consistent with SWS. **(B)** Typical MRS spectrum showing the locations of key peaks from one voxel: NAA=N-acetyl aspartate, Cr=creatine, CHO=choline, GLU=glutamate, GLN=glutamine. **(C)** Locations of voxels with calculated GLU/Cr values

(all colored voxels). Most voxels in the affected hemisphere showed higher Glu/Cr ratios than corresponding voxels in the unaffected (left) hemisphere. Maximum GLU/Cr ratios were measured in the right frontal lobe (arrow); (**D**) the same area showed increased interictal glucose metabolism on FDG-PET (arrow).

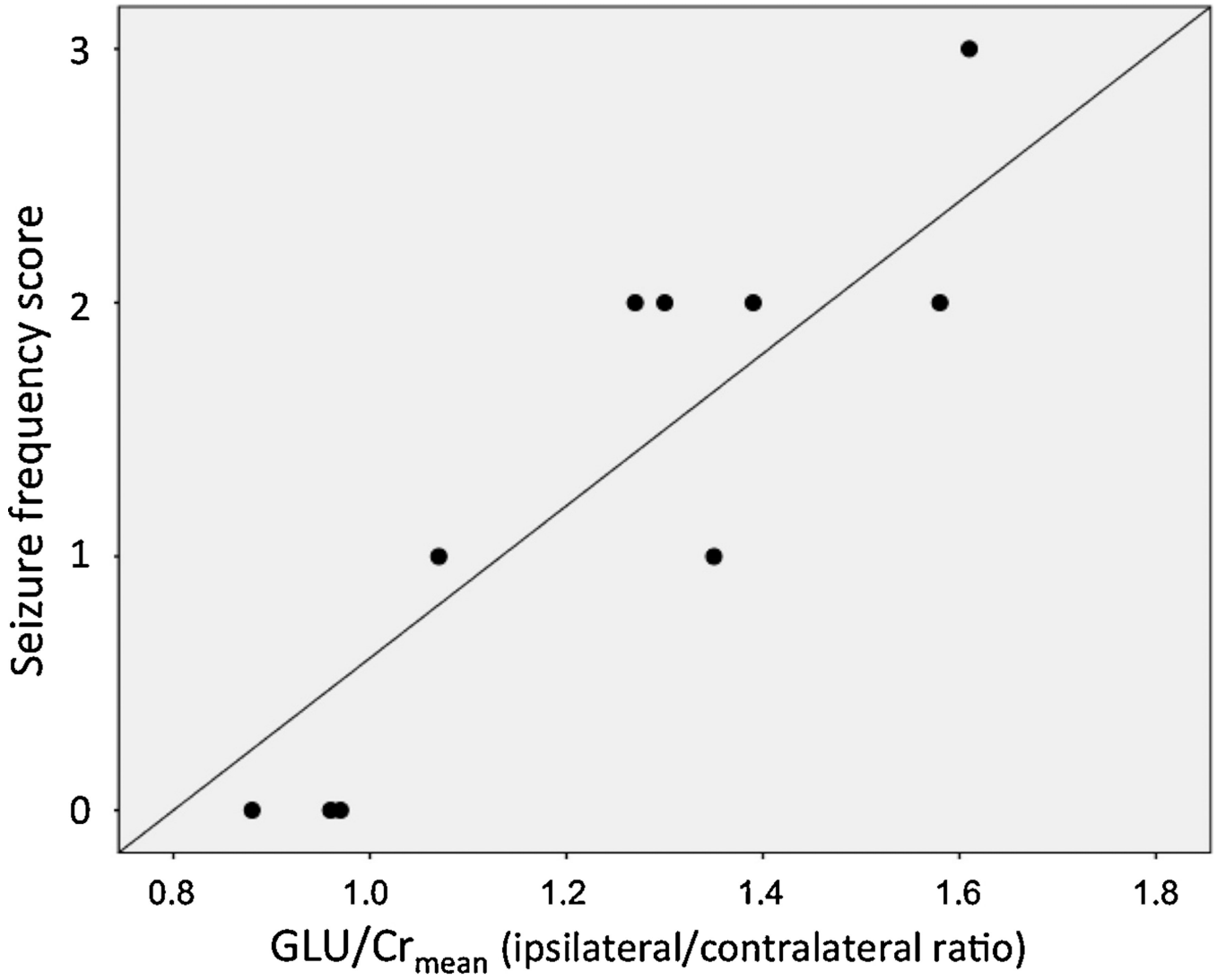

Figure 2.
Correlation between asymmetries of mean GLU/Cr (expressed as ipsilateral/contralateral ratios) and clinical seizure frequency scores.

Table 1

Clinical data of the 10 children with unilateral Sturge-Weber syndrome

Pt. No.	Gender	Age (mo)	PWS	LMA	Glaucoma	Age at epilepsy onset (mo)	Seizure type(s)	AED	Seizure frequency score		FDG-PET	EEG (at PET)
									baseline	follow-up		
1	F	7	R V1	R FTPO	no	1	IS, focal	OXC, LEV	3	2	R FTP incr	few spikes
2	F	13	R V1-3	R FTPO	no	5	focal (SE)	OXC, LEV	2	3#	R TPO decr, F incr	no epi
3	F	18	L V1-3	L FTPO	no	4	focal	OXC	0	1	L FTPO incr	no epi
4	F	20	R V1-3, L V3	R TPO	yes	5	focal	OXC, LEV	2	1	R TPO>F decr	no epi
5	F	30	L V1-2	L OT	no	4	focal	LEV	2	2#	L O>TP decr	no epi
6	F	38	R V1-2	R FTPO	yes	29	focal	OXC, GAB	1	1	R TO>FP decr (incr)*	no epi
7	M	40	R V3	R P	no	10	focal	OXC, LEV	2	2	R PO decr	no epi
8	M	44	none	R TP	no	7	focal	LEV, ZON	1	n/a	R TPO>F decr (P incr)*	no epi
9	F	65	R V1-3, L V3	R FTPO	yes	3	focal	OXC, LEV	0	0	R FTPO decr	no epi
10	F	78	L V1	L TPO	no	6	focal	PHB	0	0	L TPO>F decr	no epi

Abbreviations: F=female, M=male, mo=month(s); PWS=port-wine stain; R=right; L=left; V1-3=branches 1–3 of the trigeminal nerve innervation area; LMA=leptomeningeal angiomatosis; IS=infantile spasms; SE=history of status epilepticus; AED=antiepileptic drug; OXC=oxcarbazepine; LEV=levetiracetam; GAB=gabapentin; ZON=zonisamide; PHB=phenobarbital; asp=aspirin; n/a=not available; epi=epileptiform EEG activity

*Had increased FDG uptake on previous PET 1 year earlier but decreased FDG uptake at the time of MRSI

#Had epilepsy surgery (therefore, follow-up was <1 year: 6 months for patient #2 and 3 months for patient #5)

Table 2

Asymmetries (ipsilateral/contralateral ratios) of mean GLU/Cr and NAA/Cr, and lobar locations of voxels with the highest GLU/Cr value (GLU/Cr_{max}) in the affected hemispheres

Patient No.	Ipsilateral/contralateral ratios			GLU/Cr_{max} location
	GLU/Cr_{mean}	NAA/Cr_{mean}	GLU/Cr_{max}	
1	1.61	1.02	2.50	temporal
2	1.58	1.00	2.30	frontal
3	0.96	0.91	1.11	parietal
4	1.39	1.09	1.61	frontal
5	1.30	0.85	1.75	temporal
6	1.07	0.97	1.63	frontal
7	1.27	1.09	1.45	parietal
8	1.35	1.00	1.39	frontal
9	0.88	0.93	1.00	frontal
10	0.96	0.86	1.60	parietal
Mean	**1.24**	**0.97**	**1.63**	
SD	±0.26	±0.08	±0.47	

Table 3

Correlations between GLU/Cr and NAA/Cr asymmetries, seizure frequency scores and age

MRSI parameter	Baseline seizure frequency		Follow-up seizure frequency		Age	
	r value	p value	r value	p value	r value	p value
GLU/Cr ipsi/contra ratio	0.88	0.001	0.80	0.009	−0.64	0.048
NAA/Cr ipsi/contra ratio	0.60	0.064	0.36	0.35	−0.32	0.36